Tunable spectroscopic and electrochemical properties of conjugated *push–push*, *push–pull* and *pull–pull* thiopheno azomethines†

Stéphane Dufresne, Marie Bourgeaux and W. G. Skene*

Received 9th November 2006, Accepted 22nd December 2006
First published as an Advance Article on the web 23rd January 2007
DOI: 10.1039/b616379c

Novel azomethines consisting uniquely of thiophene units were examined. The highly conjugated compounds were prepared by condensing air stable aminothiophenes with 2-thiophene aldehydes, which were substituted with various electronic groups. The resulting azomethines are highly conjugated and are both reductively and hydrolytically resistant. Various electron donating and accepting groups placed in the 2-position of 5-thiophene carboxaldehyde lead to electronically delocalized *push–push, pull–pull*, and *push–pull* azomethines. These electronic groups affect both the HOMO and the LUMO levels, which influence the absorption and emission spectra. Colors spanning the entire visible spectrum ranging from yellow to blue are possible with these nitrogen containing conjugated compounds. Excited state deactivation of the singlet excited state occurs predominately by internal conversion while only a small amount of energy is dissipated by intersystem crossing to the triplet state and by fluorescence. The ensuing fluorescence and phosphorescence of the thiopheno azomethines are similar to those of their thiophene analogues currently used in functional devices, but with the advantage of a low triplet state and tunable HOMO–LUMO energy levels extending from 3.0 to 1.9 eV. Quasi-reversible electrochemical radical cation formation is possible while the oxidation potential is dependent on the nature of the electronic group appended to the thiophene. The crystallographic data of the electronic *push–push* system show the azomethine bonds are planar and linear and they adopt the *E* isomer.

Introduction

Conjugated materials have received much attention as they offer many new possibilities for devices combining unique optical, electrical, and mechanical properties.[1] Particular interest is found with thiophene based materials because of their low oxidation potentials[2] and their equally low band-gap properties,[3] which make them useful for many electronic devices. Moreover, these compounds show such versatility because of their semiconductor like properties obtained with chemical doping that further make them suitable for commercial applications. As a result of the diverse emissive and conductive properties and various synthetic means for their formation, conjugated thiophene materials have found many applications including uses as hole injection layers in OLED/PLEDs, in flexible light displays, solar cells, flat panel displays, field effect transistors, non-linear optical materials, sensors, and/or low power consumption products, to name but a few.[4,5]

As attractive as these conjugated materials are for their physical properties, their synthesis is however challenging. Typical synthetic methods such as Suzuki[6] and Wittig[7] strategies or electropolymerization[8] used to obtain conjugated thiophenes are often quite stringent. Alternating π-conjugated units with various electron donor and acceptor groups cannot be readily obtained by these normal coupling means. Standard synthetic means furthermore do not easily promote the selective one-pot addition of monomer units in high yields to afford unsymmetric electronic π-conjugated *push–pull* systems. Such conjugated compounds along with their electronic *pull–pull* and *push–push* analogues offer a viable means for spectroscopic property tuning and they provide a new realm of easily synthesized functional materials for enhanced emitting devices or non-linear optical materials.[9]

Azomethines (–N=CH–) are appealing alternatives for conjugated materials because of the mild reaction conditions required for their synthesis. They have the advantage of increased yields and selective addition through the condensation reaction between an amine and an aldehyde, requiring less difficult purifications. The result of the easy reaction between the two complementary groups is a robust azomethine connection that is conjugated and exhibits a high stability towards hydrolysis and reduction when aryl precursors are employed.[10–13] Research progress regarding functional azomethine materials has unfortunately not been as prolific as their carbon analogues because of the limited number of available stable aryl diamino precursors. Such precursors often undergo undesired oxidative decomposition while the resulting azomethine products do not have suitable properties for functional applications and suffer from problematic irreversible oxidation.[14,15] Only recently have efforts focused on taking advantage of these robust bonds to end cap oligomers using thiophene aldehyde precursors.[16] The recent introduction of stable aminothiophenes (**1** and **3**) have further helped to develop azomethine research leading to conjugated

Département de Chimie, Pavillon JA Bombardier, Université de Montréal, CP 6128, succ. Centre-ville, Montréal, Québec, Canada H3C 3J7. E-mail: w.skene@umontreal.ca

† Electronic supplementary information (ESI) available: experimental section; absorption and emission spectra; cyclic voltammetry; reduction analyses. See DOI: 10.1039/b616379c

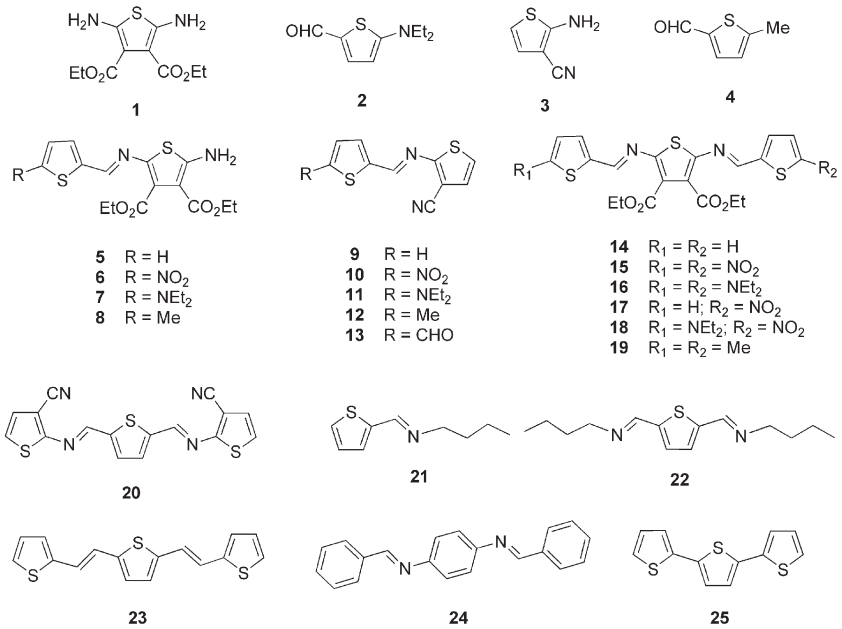

Chart 1 Conjugated azomethines examined, their precursors, and some representative carbon analogues.

azomethines consisting uniquely of thiophene units.[17,18] These extremely stable compounds do not suffer from the limitations of previous azomethines.[19] Furthermore, they have the added advantage of being isoelectronic to their carbon analogues,[20] making them suitable replacements for conventional thiophene materials.

Recently, we developed a route to synthesize oligothiopheno azomethines by selective reagent addition.[21,22] The potential advantages of azomethine-based materials concomitant with our previous success with such compounds[13] have prompted us to develop new symmetric and unsymmetric thiopheno azomethines. The main objective is to examine the physical properties, among which are the spectroscopic and photophysical properties including the cyclic voltammetry, of these new compounds. These are of particular interest giving the limited number of the photophysical and electrochemical studies regarding azomethines especially their thiophene derivatives. Herein, we present the preparation and characterization of conjugated thiopheno azomethines containing terminal electron donating and accepting groups. The sequential assembly of these electronic *push–push*, *pull–pull* and *push–pull* π-conjugated compounds is presented. The steady-state and time-resolved photophysics, electrochemical properties, HOMO–LUMO energy gaps, and crystal structures of these unique thiopheno azomethines are also investigated.

Results and discussion

Synthesis

The reaction conditions to afford the azomethines involve shifting the equilibrium by simple dehydration *via* hydroscopic solvents (*i.e.*, absolute ethanol and anhydrous toluene and THF) or mild drying agents (*i.e.*, molecular sieves and alkali sulfates). These parameters concomitant with the formation of the thermodynamically favorable conjugated products displace the equilibrium in favor of the products without the need of stringent conditions, unlike standard carbon coupling methods. The versatile reaction supports a wide variety of common organic solvents with selective product formation (Scheme 1) through the judicious choice of solvent, temperature and reagent stoichiometry. This selectivity is courtesy of the different reactivity of the amino groups of **1** in its pristine form relative to its monoazomethine form. Selective monoaddition to yield the amino monoazomethines is done with one equivalent of the corresponding aldehyde by condensing it with **1** at room temperature or by refluxing in ethanol. Both instances lead exclusively to the monoadducts, owing to the deactivation by the electron withdrawing ester group. The deactivating group is further responsible for the increased stability of **1** relative to its unsubstituted 2,5-diaminothiophene analogue, which spontaneously undergoes oxidative decomposition under ambient conditions and cannot be isolated. The electron withdrawing group is also responsible for decreasing the amine nucleophilicity. As a result, only mild reaction conditions are required for the condensation of monoazomethines. The electron withdrawing effect of the azomethine bond in the monoazomethine further reduces the amine reactivity. More stringent reaction conditions are therefore required to push the second condensation to form the bisazomethine. This provides a means to tailor product formation by changing either the reagent stoichiometry or the solvents used. The resulting azomethine bond is sufficiently robust that it resists reduction with common reducing agents such as $NaBH_4$ and resists even strong reductants including DIBAL and H_2/Pd using standard protocols. Only in the case of refluxing with DIBAL for 10 hours did reduction of the azomethine occur. Azomethine hydrolysis occurs only with prolonged heating with concentrated acid in water saturated organic solvents. No product decomposition was observed even after eighteen months in solution under normal conditions.

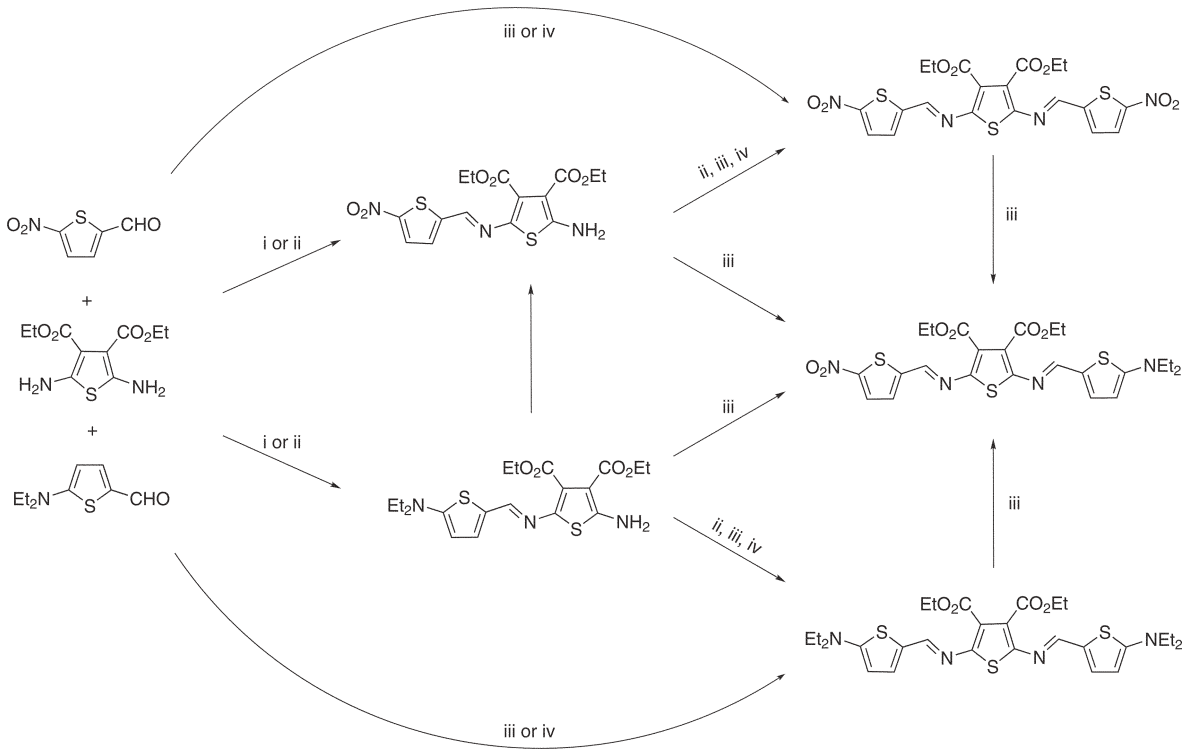

Scheme 1 Conjugated thiophene assembly by complementary precursors leading to tunable properties. Experimental conditions: i) EtOH, Δ, ii) *i*-PrOH, Δ, iii) $TiCl_4$, DABCO, toluene, Δ, iv) *n*-BuOH, Δ.

The monoazomethines **5–8** are formed exclusively in ethanol regardless of the aldehyde used and the stoichiometry employed. By simply changing the solvent polarity and using different boiling point solvents, such as isopropanol or *n*-butanol, the reaction can be pushed to afford the corresponding bisazomethines in most cases (*vide infra*). Condensation can be done sequentially in a one-pot fashion directly from **1** with two equivalents of the corresponding aldehyde. Alternatively, an additional equivalent of aldehyde can be added to **5** to afford **14**. In all cases in which controlled addition was possible, the condensation reaction was optimally catalyzed with *ca.* 5 mol% of trifluoroacetic acid. The controlled addition methodology is amenable to any aldehyde combination with **1** and provides a useful method for preparing new conjugated thiophenes. The reduced amine reactivity arising from the electron withdrawing ethyl ester group is evident with monomer **1** in which **14** can be obtained only by using high boiling point solvents, such as *n*-butanol.

Unlike **1**, selective product formation was not observed with the monoamine precursor **3**. The addition of one equivalent of **3** to 2,5-thiophene dicarboxaldehyde afforded a mixture of monoadduct **13** with a predominate amount of bisazomethine **20**. Product control with **3** was not possible even in ethanol at room temperature, which otherwise led to product control with **1**. Unlike previous examples that exploited solubility differences to afford selective product formation,[13,23] such selectivity was not observed with **3**. The lack of selectivity is attributed to the electron withdrawing cyano group that deactivates the amine and results in reduced reactivity towards the aldehyde. The cyano electron withdrawing effect of **13** increases the aldehyde reactivity towards nucleophilic addition. The unreacted amount of **3** therefore condenses preferentially with **13** immediately upon its formation resulting in the observed abundance of **20** relative to **13**.

Synthesis of the substituted bisazomethines is not straightforward owing to the different reactivity of the amino group of **1** towards the various aldehydes. The bisazomethines are obtained with mild dehydration methods only with prolonged reaction times that result in significant aldehyde decomposition. The strong electron donating character of the diethylamino group of **2** deactivates the aldehyde such that nucleophilic addition of **1** cannot be done under mild conditions. Alternatively, its reactivity can be increased with a Lewis acid such as $TiCl_4$.[24] This route significantly decreases the reaction time while improving the yields of the coupling reaction to afford conjugated monoazomethines (**7** and **11**) and bisazomethines (**16** and **18**). Conversely, the electron withdrawing nitro group of 5-nitrothiophene-2-carboxaldehyde allowed for easy azomethine formation by simple heating with an acid catalyst in isopropanol only with the amino precursors **1** and **3**. The strong electron withdrawing nature of the nitro group, the high degree of conjugation, concomitant with the ester withdrawing capacity of **6**, further reduces the amine's nucleophilic character and prevents bisazomethine formation. This explains the difficulty in forming **15**, which could be obtained only by the Lewis acid method from **1** or **6**. Since these compounds are highly conjugated, the electronic withdrawing/donating groups exert their influence throughout the entire molecule. The reactivity of the terminal amine in the monoazomethines is therefore influenced by these electronic effects.

The synthesis of the unsymmetric compounds was further challenging because of their dynamic covalent character

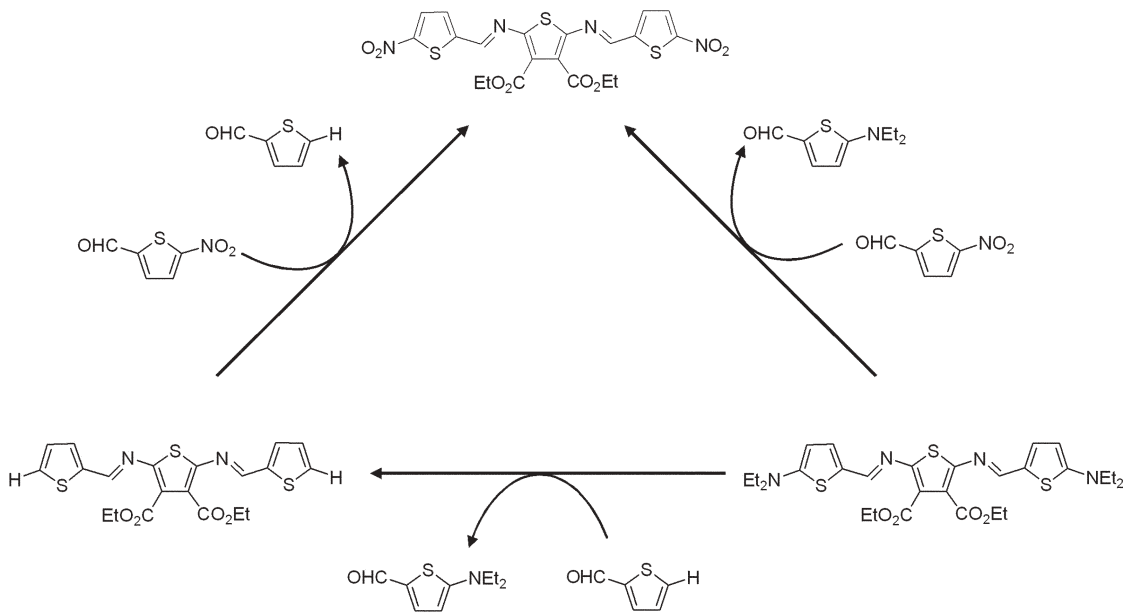

Scheme 2 Possible Lewis acid promoted dynamic component exchange of different monomers.

resulting in Lewis acid induced component exchange illustrated in Scheme 2.[25,26] Under our coupling conditions, attempts to obtain the unsymmetric **17** from **5** resulted quantitatively in **6**. Instead of undergoing the second condensation to form a bisazomethine, the terminal thiophene was exchanged with 2-nitrothiophene carboxaldehyde, according to Scheme 2. The resulting product is the thermodynamically stable **6** and its formation is consistent with previous examples of Lewis acid catalyzed component exchange.[26,27] Consequently, the synthesis of **17** was achieved by exploiting the dynamic component reaction to exchange the thiophenes under stoichiometric conditions from **14**. The 2-diethylamino thiophene can also sustain a dynamic component exchange and be replaced either by thiophene carboxaldehyde or by the 2-nitrothiophene carboxaldehyde component in the conjugated bisazomethines. Thus, as predicted by the thermodynamic stability and the reactivity of each compound, the nitrothiophene preferentially exchanges with the thiophene compound which, in turn, can displace the diethylamino thiophene unit according to Scheme 2. The advantage of this dynamic behavior is a tunable synthesis for each compound. The observed dynamic behavior assures formation of the most thermodynamically stable product, further supporting the conjugated character of the azomethine compounds. A diverse library of electronic *push–push*, *pull–pull* and *push–pull* conjugated compounds is therefore possible *via* the step-wise pathways and opens a new synthetic means of tunable materials.

Spectroscopic properties

The extent of oligomerization can visually be followed by the intense color change from yellow (**1**) to orange (**5**) and to deep red (**14**) with the unsubstituted compounds. Their pronounced bathochromic change (Fig. 1 and Table 1) is indicative of the conjugation degree arising from azomethine bond formation. The observed transitions are dominated by lowering of the excited electronic π–π* levels owing to the stabilization from increasing the degree of conjugation. The molar absorptivity coefficients are substantially high for all the azomethines because of the highly allowed π–π* transitions. The linear bathochromic shift with the reciprocal number of unsubstituted thiophene units observed (Fig. 1 inset) further supports the conjugated nature of the azomethine bond. The bathochromic shift is consistent with a planar rigid π-conjugation of the compounds. Moreover, extrapolation of the curve gives the potential absorption maximum for an azomethine polymer consisting entirely of thiophene units, being *ca.* 500 nm.

The combined spectroscopic results for the various thiopheno azomethines are reported in Table 1. The absorption and emission spectra intercept provides the relative energy

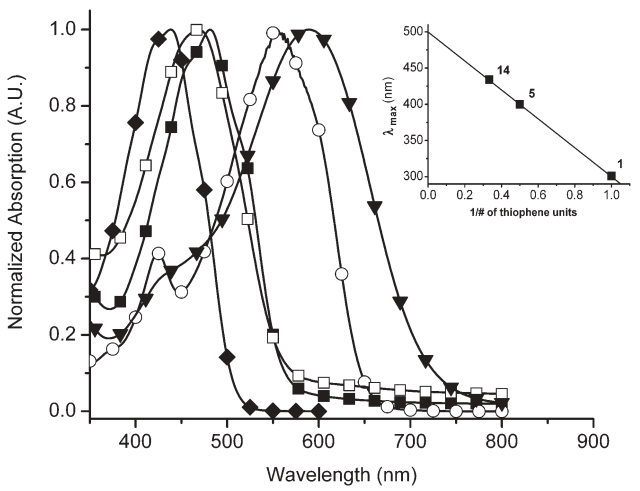

Fig. 1 Influence of terminal electronic groups on the absorption spectra of **14** (closed diamonds), **15** (closed squares), **16** (open circles), **17** (open squares), **18** (closed triangles). Inset: reciprocal number of thiophene units *versus* the change in absorption maximum for the unsubstituted thiophenes.

Table 1 Spectroscopic values for the various reagents and azomethines measured in anhydrous acetonitrile

	Module	Abs.[a]/ nm	$\varepsilon_{\lambda max}$/ M^{-1} cm^{-1}	Em.[b]/ nm	Φ_{fl}[c] ($\times 10^{-3}$)	Φ_{fl} (77 K)[d]	τ_{fl}[e]/ns	ΔE[f]/eV	E_g[g]/eV	k_r[h]/μs^{-1}	k_{nr}[i]/ ns^{-1}	Phos.[j]/ nm
Reagents	**1**	305	37 000	335	2.5	0.0089	13.5	3.7	3.0	0.19	0.08	479
	2	371	32 000	408	0.5	0.0058	0.3	3.2	3.0	1.67	3.34	543
	3	279	15 000	304	3×10^{-3}	7.7×10^{-6}	3.9	4.2	3.9	8×10^{-4}	0.27	493
	4	295	10 000	323	0.2	0.00058	4.6	4.0	3.3	0.04	0.20	500
Aminomonoazomethine	**5**	400	19 000	480	2.9	0.97	14.0	2.9	2.6	0.21	0.07	525
	6	490	29 000	637	1.2	0.89	16.7	2.3	2.0	0.07	0.06	698
	7	452	42 000	542	2.7	0.96	13.5	2.5	2.3	0.93	0.07	549
	8	404	16 000	516	2.3	0.94	1.0	2.7	2.3	2.30	1.00	530
Monoazomethine	**9**	370	14 000	439	3.9	0.79	5.4	3.2	2.7	0.72	0.18	479
	10	400	36 000	454	2.6	0.68	5.8	2.9	2.5	0.45	0.17	536
	11	473	49 000	545	8.7	0.82	11.1	2.4	2.3	0.78	0.09	578
	12	379	17 000	451	1.3	0.68	0.5	2.9	2.7	2.60	2.00	520
	13	385	22 000	426	1.5	0.72	1.5	3.0	2.6	1.00	0.67	481
Bisazomethine	**14**	440	64 000	534	2.8	0.71	13.2	2.6	2.3	0.21	0.07	560
	15	481	37 000	589	1.6	0.15	11.9	2.4	2.1	0.13	0.08	600
	16	555	34 000	659	1.9	0.95	16.6	2.0	2.0	0.11	0.06	751
	17	470	30 000	614	5.6	0.70	14.1	2.3	2.1	0.40	0.07	695
	18	588	45 000	660	2.1	0.51	9.3	1.9	1.6	0.23	0.11	686
	19	427	46 000	559	1.3	0.90	1.9	2.5	2.2	0.68	0.52	598
	20	451	65 000	500	1.4	0.56	2.1	2.6	2.3	0.67	0.48	575
Model compounds	**21**	277	24 000	306	0.2	0.76	4.3	4.2	3.8	0.05	0.25	481
	22	312	27 000	344	0.6	0.50	1.6	3.7	3.5	0.38	0.63	490
	23[k]	423	—	—	40	—	1.8	2.5	2.4	22	0.53	—
	24	376[l]	28 400[l]	—	—	—	—	—	—	—	—	—
	25	351[m]	24 000[n]	422[m]	56[n]	—	0.2[n]	3.2[o]	3.1[o]	280	4.72	—

[a] Absorption maximum. [b] Emission maximum. [c] Fluorescence quantum yields at λ_{ex} = 303 nm, relative to bithiophene.[30] [d] Fluorescence quantum yields at 77 K relative to room temperature. [e] Monoexponential fluorescence lifetime measured at λ_{em} max. [f] Absolute HOMO–LUMO spectral difference. [g] Spectroscopic band-gap. [h] $k_r = \Phi_{fl}/\tau_{fl}$. [i] $k_{nr} = k_r(1 - \Phi_{fl})/\Phi_{fl}$. [j] Phosphorescence measured in 1 : 4 methanol–ethanol matrix at 77 K. [k] From Frère and coworkers.[57] [l] From Gawinecki and Muzalewski,[58] and Coville and Neuse.[59] [m] From Seixas de Melo and coworkers.[30–32,35] [n] From Roncali and coworkers.[57] [o] From Marks and coworkers.[60]

difference between the ground and the excited states.[28] From the combined normalized absorption–emission spectra, the relative HOMO–LUMO transition can be calculated from the spectral overlap. The absorption method further provides an estimate for the band-gap that can be derived from the absorption onset in the red region of the spectrum. This method applies to our compounds since only a slight bathochromic shift of *ca.* 20 nm between solution and thin film was observed. The measured values by this method show the azomethines possess lower band-gaps relative to their carbon analogues such as **23** and **25**. The similarity of the azomethines to structurally comparable nitrogen free thiophenes is evident from the photophysical data presented in Table 1. The electronic groups chosen are known to influence both the HOMO and LUMO levels, which is evident from the spectroscopic data. In general, the electron donating and the electron withdrawing groups are known to decrease the HOMO and increase the LUMO levels, respectively. Such perturbations translate into apparent energy gap differences and intense absorption and emission spectral variations.

The monoazomethines **9–13** serve as reference compounds to illustrate the effect of the electronic groups. The amine group greatly affects both the absorption and the emission compared to the nitro group. This is supported by the pronounced spectral shifts of 100 nm for the donor group and only slight shifts of 30 nm for the acceptor group, relative to the reference compound **9**. The similar spectroscopic properties of the methylated analogue **9** and **12** confirm the pronounced spectroscopic change is a result of the electronic groups. The same tendency is observed also with the amino monoazomethines (**5–8**) whose terminal $-NH_2$ further influences the properties *via* its donating character. The electronic terminal groups can collectively influence the resulting properties courtesy of the highly conjugated azomethine bond. The withdrawing $-NO_2$ and donating $-NH_2$ of **6** jointly stabilize the ground and excited states, respectively, leading to an electronic *push–pull* system. This results in pronounced bathochromic absorption and emission shifts relative to **5**. Only slight bathochromic shifts are observed with **7** because of the two amino groups that work in opposition leading to an electronic *push–push* system.

The bisazomethines exhibit the same spectroscopic trend as the monoazomethines. Both the absorption and the emission spectra of the bisazomethine undergo large bathochromic shifts relative to the monoazomethines because of the increased conjugation. The pronounced stabilization implies a high degree of delocalization and planarity throughout the azomethines. The electronic group cooperativity is more pronounced for the bisazomethines than for the monoazomethines, supported by the spectral differences observed for **15–18** relative to the unsubstituted **14**. The *push–push* compounds **15** and **17** exhibit slight spectral shifts of 40 nm while the corresponding amino substituted *pull–pull* compound undergoes a large bathochromic shift around 70 nm, relative to **14**. The electronic *push–pull* system (**18**), combining both a donor and an acceptor group, exhibits the most pronounced absorption and emission bathochromic shifts. The *push–pull* effect greatly perturbs the electronic transitions and reduces the HOMO–LUMO energy gap between the ground and excited states. The net outcome is an intense visible blue color

for **18** in addition to an extremely low HOMO–LUMO energy gap of 1.9 eV. From these observations, it can be concluded that the donating group has a greater effect on the electronic transitions than the nitro group, supported by the pronounced bathochromic shifts. This is concomitant with the ester groups on the thiophene central ring that also influence the spectroscopic properties through their withdrawing character. Thus, depending on the substituent chosen, it is possible to tailor the electronic properties of a given bisazomethine by perturbing either the HOMO or LUMO energy levels.

The influence of the nitrogen placement within the azomethine bond upon the resulting spectroscopic properties was examined with model compounds **14** and **20**. The spectroscopic properties, including HOMO–LUMO energy gap and molar absorption coefficients, of these two compounds are very similar, which confirms the comparable withdrawing effect of the cyano and the ester groups upon the electronic transitions. This is further supported by the similar spectroscopic results for the analogues **9** *versus* **12** and **14** *versus* **19**. The placement of the nitrogen within the azomethine bond does not perturb the electronic transitions given the comparable spectroscopic results among the studied compounds. Conversely, the nature and the number of substituents in the 5 and 5′ positions (Fig. 2) greatly affect the electronic transitions which, in turn, influence the absorption and emission spectra in addition to the HOMO–LUMO energy gap.

Steady-state and time-resolved fluorescence measurements further provide valuable insight into the excited state deactivation pathways of these compounds. Both the similar ns fluorescence lifetimes and the calculated radiative rate constants (k_f) for all the azomethines imply similar deactivation modes of the singlet excited state for all the compounds. The monoexponential lifetimes suggest unimolecular deactivation which is further supported by the dilute experimental conditions, which preclude bimolecular self-quenching. The low fluorescence quantum yields are indicative of nonradiative quenching deactivation processes such as intersystem crossing (ISC) to the triplet state or by internal conversion (IC). Photoisomerization between the *E* and the *Z* isomers is also a possible deactivation mode.[29] However, no such photoproducts were observed. The low fluorescence quantum yield for the thiopheno azomethines is however not surprising since thiophenes are known to weakly fluoresce because of efficient ISC to the triplet state. This is understood to occur by heavy atom induced spin–orbit coupling by the sulfur atoms.[30–35] This behavior is expected to be enhanced further by the azomethine nitrogen that contributes to the heavy atom effect concomitant with the increased degree of conjugation, which favors ISC by narrowing the singlet–triplet gap. Population of the triplet manifold is supported by the phosphorescence measurements at 77 K that show a bathochromic emission

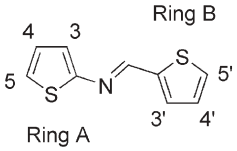

Fig. 2 Numbering scheme of thiopheno azomethines.

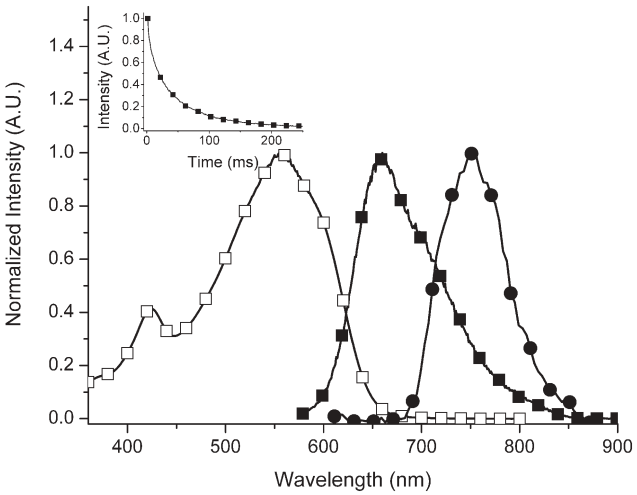

Fig. 3 Normalized absorption (open squares) and fluorescence (closed squares) spectra of **16** in acetonitrile. Phosphorescence (closed circles) spectrum measured in 4 : 1 ethanol–methanol matrix at 77 K. Inset: phosphorescence decay monitored at 760 nm.

relative to the fluorescence and a monoexponential emission decay (Fig. 3). The phosphorescence quantum yields at this low temperature can be calculated by relative actinometry with fluorenone.[36] The phosphorescence quantum yields measured for all the studied compounds are approximately the same, $\Phi_{phos} \leqslant 0.1$. The triplet energies can be calculated from the $E(0,0)$ transition from the phosphorescence spectra and these values are comparable to those of **23** and **25**.[33,37]

Further evidence of the triplet state is provided by ns-laser flash photolysis (LFP) from the weakly absorbing transients observed at 280 and 370 nm for the monoazomethine and bisazomethine, respectively (Fig. 4). The transients produced by the intense laser pulse are assigned to the triplets owing to their monoexponential decay kinetics that are similar to benzophenone (Fig. 4 inset) in addition to being quenched with standard triplet quenchers such as oxygen, 1,4-cyclohexadiene,

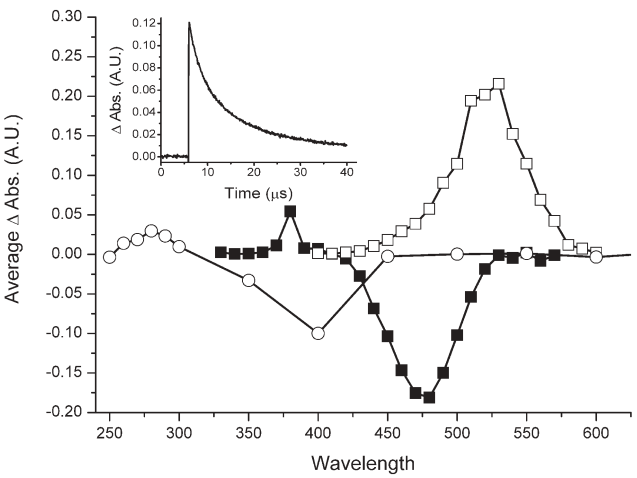

Fig. 4 Transient absorption spectra of benzophenone (open squares), **6** (open circles), and **17** (closed squares) recorded 100 μs after the laser pulse at 266 nm in deaerated acetonitrile. Inset: the decay of triplet benzophenone recorded at 525 nm.

β-carotene, and methylnaphthalene.[38] Also apparent in the transient absorption spectra are negative absorptions resulting from the strong ground state bleaching of the azomethines. These are mirror images of the ground state absorption spectra and confirm the transient absorption is much weaker than the ground state absorption. Even though there is direct evidence for the triplet state by LFP, this manifold is not preferentially formed and therefore it is not responsible for deactivating the singlet state. This is derived from the surprisingly weak azomethine transient signal. Large triplet extinction coefficients (ε_T) $\geqslant$10 000 M^{-1} cm^{-1} are assumed for the azomethines because of their high degree of conjugation.[39] Owing to the intense ε_T, a transient signal of equal intensity to that of benzophenone (ε_T = 8 400 M^{-1} cm^{-1}, Φ_T = 1) is expected if the azomethine triplet is produced in significant amounts. Since both Φ_T and ε_T contribute to the LFP signal, the weak azomethine signal obtained under identical experiment conditions as benzophenone (Fig. 4) confirms the azomethine triplet formation is inefficient. An upper limit of $\Phi_T \approx 0.05$ is derived from the LFP signal relative to benzophenone and is in agreement with the phosphorescence quantum yields. Evidence for the low triplet efficiency of the azomethines is further supported by the calculated nonradiative rate constants (k_{nr}) that are greater than **25**, which is known to efficiently populate its triplet state.[31] The faster k_{nr} values taken together with the weak LFP signal implies that deactivation of the singlet state occurs predominately by nonradiative IC and not by a manifold shift to the triplet state as with conventional thiophenes.

Evidence for the IC deactivation mode is confirmed by the relative fluorescence at 77 K that is two and half orders of magnitude greater than that at room temperature (Fig. 5). All modes of excited state deactivation involving bond rotation and diffusion controlled quenching processes are suppressed at this low temperature leading to Φ_{fl} (77 K) ranging between 0.53 and 0.97 for the compounds studied. Accurate values for the low temperature fluorescence yields cannot be derived because of experimental errors associated with calculating the weak fluorescence signal at room temperature relative to the intense one at 77 K. Nonetheless, the observed fluorescence signal decrease at room temperature is from efficient nonradiative deactivation of the singlet excited state by IC according to Φ_{fl} (77 K) − Φ_{fl} (RT) ≈ Φ_{IC}. This is in contrast to conventional oligothiophenes, such as **25**, that efficiently populate their triplet state by ISC with $\Phi_T \geqslant 0.8$.[30–32] Even though the major deactivation pathway is by IC, a certain amount of the excited state energy remains unaccounted for according to the following energy conservation equation: $\Phi_{fl} + \Phi_{ISC} + \Phi_{IC} \approx 1$. The residual excited state energy must be dissipated by ISC to the triplet. Since only a weak signal is seen by LFP, the imine bond must therefore be a good triplet deactivator leading to rapid and efficient intramolecular self-quenching of this excited state.

Cyclic voltammetry

Thiophene azomethines undergo two detectable step-wise oxidations by cyclic voltammetry. The first oxidation corresponds to a one electron process from the thiophene to form a radical cation. This is followed by removal of an additional electron to form a dication. Even through the specific thiophene unit that undergoes oxidation cannot be unambiguously assigned, the first oxidation process consistently occurs between 0.4 and 1.6 V and is greatly affected by the electronic groups. Furthermore, the first oxidation step is quasi-reversible (Fig. 6) unlike homologous aryl azomethines that exhibit irreversible behavior regardless of the scan rate and experimental conditions.

In addition to an oxidation process, the azomethine bond can potentially be reduced. This process normally involves two rapid and undistinguishable sequential steps each involving one electron transfer.[40,41] However, no such processes were observed for any of the studied azomethines either in dichloromethane or at large negative potentials in DMF. This is in accordance with other reductive imine studies[42,43] and supports the observed robustness of the conjugated azomethine bond towards chemical reductants. A reversible six electron reduction was however observed for **6**, **10**, **15**, **17**, and **18**, which is assigned to the reduction of the nitro group.

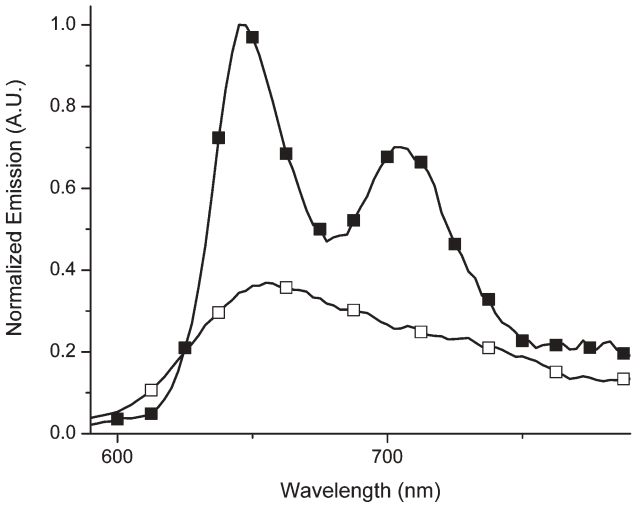

Fig. 5 Fluorescence of **15** at 77 K (closed squares) relative to room temperature (open squares, magnified 50 times).

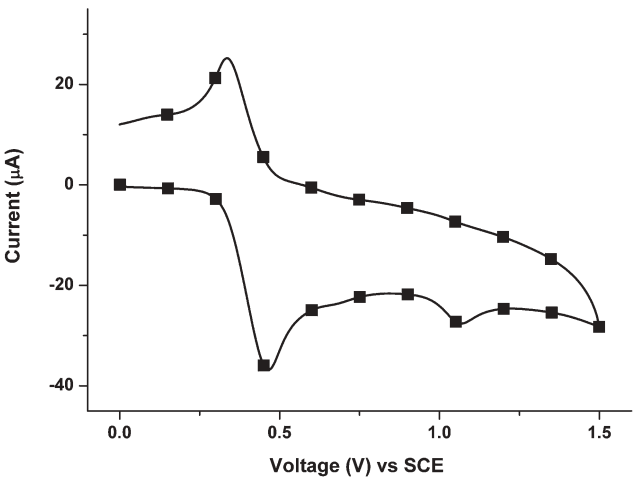

Fig. 6 Typical cyclic voltammogram of **16** in anhydrous dichloromethane at 100 mV s^{-1} with 0.1 M NBu_4PF_6 as an electrolyte.

Conversely, an irreversible reduction was observed at low potentials only for **13** and **20**. Chemical reduction of these two compounds was also possible with $NaBH_4$. The irreversible process is most likely from cyanide ion formation followed by complete thiophene decomposition.[44] NMR product studies support this in which no thiophene or azomethine is detectable after the chemical reduction of **13** and **20** with $NaBH_4$ in methanol and at room temperature.

The ability of the electronic groups to modify the HOMO/LUMO levels is apparent from the measured oxidation potentials. The donating amino group increases the HOMO level, resulting in a decrease in the oxidation potential. On average, a 500 mV reduction in the oxidation potential was observed for the amino containing compounds relative to their unsubstituted analogues. A pronounced reduction in the oxidation potential is apparent with the *push–push* system **16** where the two amino groups combine to increase the HOMO level. Unfortunately, the ability of the withdrawing group to decrease the LUMO level is not apparent since the reduction potentials cannot be measured. This notwithstanding, an increase in the oxidation potential was observed for the nitro containing thiophenes and suggests a destabilization of the HOMO level. The measured HOMO/LUMO values and how they are influenced by the electronic groups are consistent with the spectroscopic measurements.

The oxidation onset provides the ionization potential (IP) according to IP = E^{ox}_{onset}(SCE) + 4.4, where E^{ox}_{onset}(SCE) is the oxidation potential onset in volts *versus* the SCE electrode.[45] The ionization potentials are obtained from the measured oxidation potentials by applying a 0.39 V correction factor. Similarly, the LUMO values are calculated from the electron affinity (EA) given by the reduction onset potential (E^{red}_{onset}) according to EA = E^{red}_{onset}(SCE) + 4.4. Since no apparent azomethine electrochemical reduction was observed under our experimental conditions, the electrochemical oxidation onset and the spectroscopically measured HOMO–LUMO energy gaps can be combined to calculate the LUMO energy level according to LUMO = HOMO − E_g. The resulting values are reported in Table 2. The oxidation potential taken together with the spectroscopic E_g data provide an accurate representation of the HOMO–LUMO energy levels. The resulting energy diagram shown in Fig. 7 illustrates the perturbation effect of the various electronic groups upon the HOMO and LUMO energy levels. Since the oxidation potential for quasi-irreversible processes is dependent upon the scan rate and hence the calculated HOMO energy level, the cyclic voltammetry measurements of all the compounds were performed under identical scan rates. In general, the azomethine oxidation potentials and their HOMO–LUMO energy gaps can be modulated such that they are similar to their carbon analogues (**23** and **25**)[46] and lower than their aryl azomethine homologues (**24**), making them compatible for use in functional devices. Moreover, the HOMO level can be tailored courtesy of the electronic groups such that the energy levels are compatible with that of ITO in OLEDs, thus making these compounds potential hole injection layers in working devices.

Compounds **21** and **22** were synthesized as models to systematically assign the effect of the simple azomethine and the electronic groups on the oxidation potentials. These model compounds also help to deconvolute the azomethine oxidation processes, which have only been partially examined to date.[10,43,47] The oxidation potentials of **21** and **22** are mutually identical and they are similar to the other thiopheno azomethines. This implies the simple azomethine bond exerts little effect on the oxidation potentials of the thiophenes.[2,3,5,48] Rather, the oxidation potentials are influenced uniquely by the

Table 2 Cyclic voltammetry[a] values for the various thiopheno azomethines measured in anhydrous acetonitrile

	Module	$E_{pa}{}^1$/V	$E_{pa}{}^2$/V	$E_{pc}{}^1$/V	$E_{pc}{}^2$/V	$E_{pa(poly)}$/V	HOMO/−eV	LUMO/−eV
Reagents	**1**	0.6	1.1	—	—	—	4.9	1.2
	2	1.0	—	—	—	1.6	5.3	2.1
	3	1.3	—	—	—	—	5.7	1.5
	4	1.2	1.7	−0.7	—	—	5.6	1.6
Aminomonoazomethine	**5**	1.0	1.4	—	—	1.6	5.4	2.5
	6	1.1	—	−0.7	−1.1	—	5.5	3.2
	7	0.4	1.0	—	—	—	4.7	2.2
	8	0.8	—	—	—	—	5.1	2.4
Monoazomethine	**9**	0.9	—	—	—	1.7	5.2	2.0
	10	1.3	—	−0.6	−0.9	—	5.6	2.7
	11	0.7	1.7	—	—	—	5.0	2.6
	12	1.2	—	—	—	—	5.5	2.6
	13	1.2	—	−1.0	−1.3	—	5.5	2.5
Bisazomethine	**14**	1.0	1.3	—	—	0.7	5.1	2.5
	15	1.1	1.6	−0.5	−1.0	—	5.4	3.0
	16	0.4	1.1	—	—	—	4.7	2.7
	17	1.0	1.4	−0.6	−1.2	—	5.3	3.0
	18	0.7	1.4	−0.7	−1.1	2.1	5.0	3.1
	19	0.9	1.1	—	—	—	5.2	3.0
	20	1.2	—	−0.9	−1.2	—	5.5	2.9
Model compounds	**21**	1.0	—	—	—	1.4	5.3	1.1
	22	1.0	—	—	—	—	5.3	1.6
	23[b]	0.9	—	—	—	—	—	—
	24	1.5[c]	—	—	—	—	—	—
	25	1.1[d]	—	—	—	—	—	—

[a] Values reported are against a Ag/AgCl (sat'd) reference electrode done in CH_2Cl_2 and a scan rate of 100 mV s^{-1}. [b] From Frère and coworkers.[57] [c] From Rao *et al.*[41] [d] From Roncali and coworkers.[57]

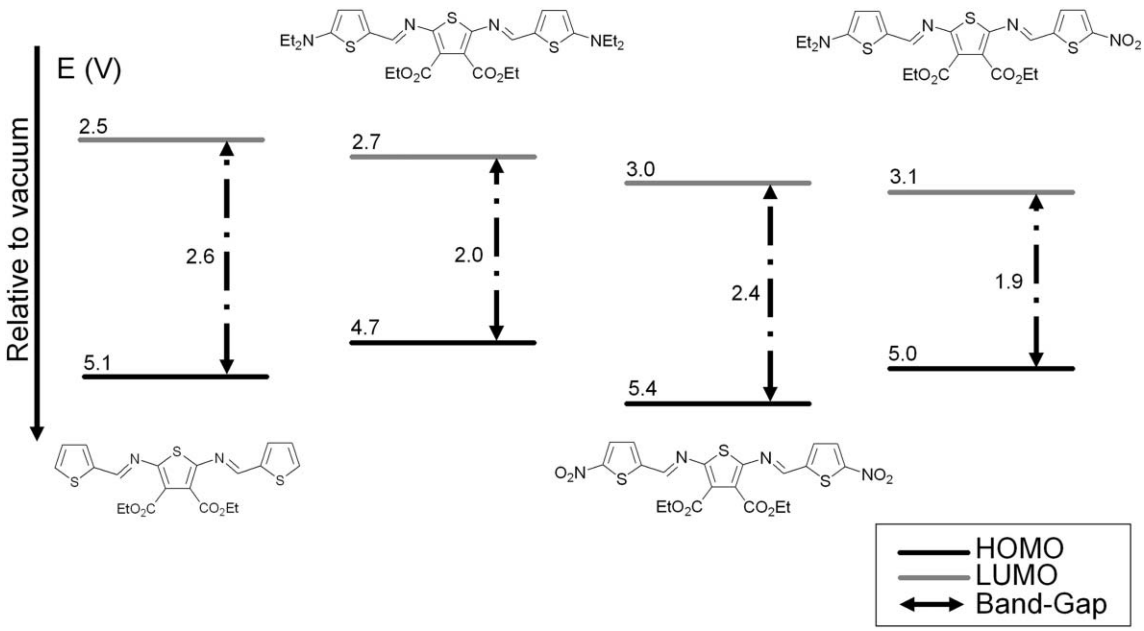

Fig. 7 Schematic representation of the relative HOMO–LUMO energy gaps influenced by different terminal electronic groups.

electronic groups and the degree of conjugation. Unlike with other thiopheno azomethines, **21** undergoes irreversible oxidation resulting from radical cation coupling to form a dimer. The product eventually is deposited as a thin film on the working electrode upon prolonged oxidation times. Conversely, the one electron oxidation to generate the radical cation is quasi-reversible for **22** and represents one of only a few examples of azomethine quasi-reversible oxidation. The reversible-like behavior is a result of substitution in the 5 and 5′ positions (Fig. 2) that prevents coupling between radical cations. This suggests that product formation occurs predominately *via* these two positions. The quasi-reversible radical cation formation is in contrast to other azomethines that undergo irreversible oxidation regardless of substitution, scan speeds, and experimental conditions because of the extremely reactive radical cation.[49] Dimer formation by oxidative coupling was observed only for the compounds that possess one substitution in either the 5 or 5′ positions.[2,50] Conversely, electrochemically induced polymerization was possible only with **14** owing to its unsubstituted 5,5′ positions.[22]

To further verify the observed irreversible oxidation was a result of radical cation coupling *via* the α,α positions, compounds **8**, **12** and **19** were examined. The terminal methyl groups of these model compounds suppress α–α oxidative coupling *via* the 5,5′ positions, but do not prevent any β–β coupling defects *via* the 3, 3′, 4, and 4′ positions. No electrochemically induced oxidative product coupling was observed for these compounds, while they exhibit reversible one electron oxidation. The lack of coupling products for **8** and **12** suggest coupling of the radical cations occurs exclusively on the thiophene Ring B (Fig. 2) and not on Ring A, to which the amine is directly bound. This may be from the electron withdrawing ester that increases the oxidation potential of thiophene A such that the oxidation occurs preferentially on Ring B. Furthermore, no significant difference was observed for the oxidation potentials of **8**, **12**, and **19** relative to their unalkylated analogues **5**, **9**, and **14**, respectively. This suggests that simple alkylation does not affect the oxidation potential. The absence of significant differences in the oxidation potentials validates the irreversible process for azomethine oxidation and confirms that the coupling of intermediates occurs preferentially by α–α coupling *via* the 5,5′ positions. This is further supported by the lack of coupling products with monoazomethines **10–13** along with the previous electrochemical polymerization of an alkylated derivative of **14**.[22]

Crystal structure

Similar to the carbon analogues, two geometric azomethine isomers are possible; *E* and *Z*. Unlike their carbon analogues, differentiation between the two azomethine isomers is difficult by ^{1}H-NMR. The NMR spectra of all the azomethines studied showed exclusively one imine peak in the 8–9 ppm region confirming the exclusive formation of one isomer, which is assumed to be the more thermodynamically stable *E* isomer. The crystal structures obtained for **5**,[51] **14**[52] and **16** are all consistent and confirm that both azomethine bonds in these structures adopt the *E* configuration. To confirm the *E* isomer did not preferentially crystallize, NMR spectra of the crystals used for X-ray diffraction and the mother liquor were both measured and they yielded identical ^{1}H-NMR spectra. This is further corroborated by repeated crystallization of various compounds from Chart 1 that consistently yielded the same crystal structure. Accurate correlation between the solid state and solution structures can be assumed because similar absorption spectra were observed for samples both in solution and in thin film. The latter are known to increase the planarity of twisted molecules leading to increased conjugation resulting in bathochromic shifts in the absorption spectra.

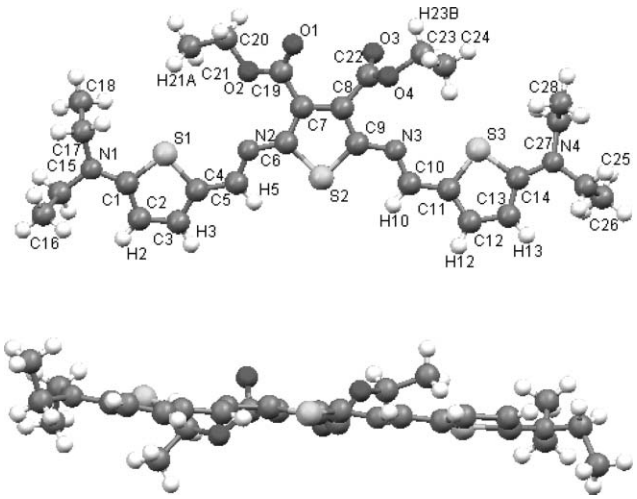

Fig. 8 Schematic representations of the crystal structure of **16**, top view (top) and seen along the *a* crystal lattice parallel to the thiophene units (bottom).

The crystal structure of **16**,‡ represented in Fig. 8, clearly shows the heteroatom units adopt an anti-parallel arrangement. The same anti-parallel arrangement of the sulfur atoms was also observed with other monoazomethines and bisazomethines.[17,51,53] The added advantage of the anti-parallel conformation and the resulting linearity confers a high degree of conjugation and validates the spectroscopic results. This arrangement is also ideal for providing high conductivities that are expected with doping.[17] The average mean planes of the terminal thiophenes were found to be twisted 5.8° and 10.6° from the mean plane of the central thiophene and its two azomethine bonds. The low twisting angle provides a planar and linear configuration to the molecule. The measured mean plane angles for **14** and **16** are in contrast to homoaryl azomethines that have twisted mean planes varying between 55° and 65° from the central thiophene.[12,14,54] A 45° angle between the two thiophene mean planes is also apparent with azomethines derived from thiophene dicarboxaldehyde such as **24**.[13,23,55] The deviation from planarity is required for the homoaryl azomethines to avoid steric hindrance between the ortho hydrogen on the homoaryl ring and the azomethine hydrogen, which are separated only by 2.16 Å.[13,55] A high degree of intramolecular hydrogen bonding and intermolecular π-stacking further contribute to the observed planar structures. This is evident from the four contacts present for **16** involving H5···S2, H10···S2, H27A···S3, and H17A···S1. There exists also a CH···O intermolecular hydrogen bond between C17–H17···O1 [$i = (-x, -y, -z)$]. The geometric parameters of this arrangement are H···O 2.34 Å, C···O 3.198(12) Å, C–H···O 141° and the pairs are linked by an inversion center to form dimers. The crystallographic data furthermore show the azomethine bond distances to be shorter than those of its carbon analogue (Table 3), which are in part responsible for the increased planarity and high degree of conjugation.[56]

‡ *Crystal data*: $C_{28}H_{30}N_4O_4S_3$, M = 588.79, triclinic, $P\bar{1}$, a = 10.5863(4), b = 10.9741(4), c = 14.5969(5) Å, α = 96.217(2), β = 97.195(2), γ = 111.441(2)°, U = 1544.06(10) Å^3, T = 100(2) K, Z = 2, μ = 2.508 mm^{-1}, 18808 reflections measured, 2540 unique (R_{int} = 0.056), $R1$ = 0.1054, w$R2$ = 0.2912 ($I > 2\sigma(I)$). CCDC reference number 626758. For crystallographic data in CIF or other electronic format see DOI: 10.1039/b616379c

Conclusion

The first examples of electronic *push–push*, *pull–pull* and *push–pull* conjugated thiophene azomethines were presented. The formation of the highly conjugated azomethine bond is responsible for displacing the equilibrium in favor of reductively and hydrolytically resistant new materials. Through the selective synthesis, different substituents and electronic groups can be incorporated into the conjugated framework leading to symmetric and unsymmetric compounds. These electronic groups provide a means to control the physical properties such as HOMO–LUMO energy gap, absorption, and color emission because of the inherent conjugation of the azomethine bond that allows perturbation of the HOMO and LUMO energy levels. The spectroscopic and electrochemical properties can be tailored by varying the number of thiophene units and the nature of the electronic groups substituted on the thiophenes. Reversible-like oxidation behavior and low potentials make these azomethines suitable for p-type doping while their linear and planar conformations impart a high degree of conjugation. Such properties are particularly useful because they permit fine-tuning of the various properties of the products formed. This, in turn, allows for a myriad of possibilities in the application of these compounds to meet the needs of the electronics industry, which is not easily achieved using conventional materials.

Acknowledgements

The authors acknowledge financial support from the Natural Sciences and Engineering Research Council Canada, Fonds de Recherche sur la Nature et les Technologies, the Centre for

Table 3 Selected crystallographic data of thiophene azomethines and a carbon analogue

		14[b]		**16**		**23**[c]	
	5[a]	Side A	Side B	Side A	Side B	Side A	Side B
Plane angle[d]	7.3°	9.1°	25.3°	10.6°	5.8°	0°	6°
–C=N–[e]	1.283 Å	1.277 Å	1.286 Å	1.296 Å	1.282 Å	1.278 Å	1.439 Å
=N–Aryl–[e]	1.351 Å	1.381 Å	1.393 Å	1.363 Å	1.374 Å	1.585 Å	1.312 Å
=CH–Aryl–	1.426 Å	1.443 Å	1.435 Å	1.432 Å	1.418 Å	1.614 Å	1.430 Å

[a] From Skene *et al.*[51] [b] From Dufresne *et al.*[52] [c] From Zobel.[56] [d] Refers to the mean plane angle between the central thiophene and the terminal thiophene units. [e] For **23**, the value refers to the –C=C– bond distance.

Self-Assembled Chemical Structures, and Canada Foundation for Innovation. Gratitude is extended to Dr M. Simard for assistance with the crystal structure analyses and to Prof. D. Zargarian for helpful suggestions. M.B. thanks the Université de Montréal for a graduate scholarship.

References

1 (*a*) C. D. Dimitrakopoulos and P. R. L. Malenfant, *Adv. Mater.*, 2002, **14**, 99–117; (*b*) L. Rupprecht, *Conductive Polymers and Plastics in Industrial Applications*, Society of Plastics Engineers/ Plastics Design Library, Brookfield, CT, 1999.
2 K. A. Hansford, S. A. P. Guarin, W. G. Skene and W. D. Lubell, *J. Org. Chem.*, 2005, **70**, 7996–8000.
3 J. Roncali, P. Blanchard and P. Frère, *J. Mater. Chem.*, 2005, **15**, 1589–1610.
4 (*a*) S. J. Toal, D. Magde and W. C. Trogler, *Chem. Commun.*, 2005, 5465–5467; (*b*) J. A. Rogers, Z. Bao, K. Baldwin, A. Dodabalapur, B. Crone, V. R. Raju, V. Kuck, H. Katz, K. Amundson, J. Ewing and P. Drzaic, *Proc. Natl. Acad. Sci. U. S. A.*, 2001, **98**, 4835–4840; (*c*) T. W. Kelley, P. F. Baude, C. Gerlach, D. E. Ender, D. Muyres, M. A. Haase, D. E. Vogel and S. D. Theiss, *Chem. Mater.*, 2004, **16**, 4413–4422.
5 I. F. Perepichka, D. F. Perepichka, H. Meng and F. Wudl, *Adv. Mater.*, 2005, **17**, 2281–2305.
6 S. Beaupré and M. Leclerc, *Macromolecules*, 2003, **36**, 8986–8991.
7 A. Drury, S. Maier, M. Rüther and W. J. Blau, *J. Mater. Chem.*, 2003, **13**, 485–490.
8 A. Lima, P. Schottland, S. Sadki and C. Chevrot, *Synth. Met.*, 1998, **93**, 33–41.
9 (*a*) J. F. Lamère, P. G. Lacroix, N. F. J. M. Rivera, R. Santillan and K. Nakatani, *J. Mater. Chem.*, 2006, **16**, 2913–2920; (*b*) J. Casado, M. C. R. Delgado, M. C. R. Merchán, V. Hernández, J. T. L. Navarrete, T. M. Pappenfus, N. Williams, W. J. Stegner, J. C. Johnson, B. A. Edlund, D. E. Janzen, K. R. Mann, J. Orduna and B. Villacampa, *Chem.–Eur. J.*, 2006, **12**, 5485–5470; (*c*) M. M. C. Oliva, J. M. M. M. Raposo, A. M. C. Fonseca, H. Hartmann, V. Hernandez and J. T. Lopez Navarrete, *J. Org. Chem.*, 2006, **71**, 7509–7520.
10 O. Thomas, O. Inganäs and M. R. Andersson, *Macromolecules*, 1998, **31**, 2676–2678.
11 S. C. Ng, H. S. O. Chan, P. M. L. Wong, K. L. Tan and B. T. G. Tan, *Polymer*, 1998, **39**, 4963–4968.
12 C.-J. Yang and S. A. Jenekhe, *Macromolecules*, 1995, **28**, 1180–1196.
13 W. G. Skene and S. Dufresne, *Org. Lett.*, 2004, **6**, 2949–2952.
14 F.-C. Tsai, C.-C. Chang, C.-L. Liu, W.-C. Chen and S. A. Jenekhe, *Macromolecules*, 2005, **38**, 1958–1966.
15 C.-J. Yang and S. A. Jenekhe, *Macromolecules*, 1995, **28**, 1180–1196.
16 N. Kiriy, V. Bocharova, A. Kiriy, M. Stamm, F. C. Krebs and H.-J. Adler, *Chem. Mater.*, 2004, **16**, 4765–4771.
17 W. G. Skene, *Polym. Prepr. (Am. Chem. Soc., Div. Polym. Chem.)*, 2004, **45**, 252–253.
18 (*a*) S. Dufresne and W. G. Skene, *Polym. Mater.: Sci. Eng.*, 2005, **92**, 16–17; (*b*) W. G. Skene, *World Pat.*WO 2005073265, 2005.
19 C.-H. Huang, N. D. McClenaghan, A. Kuhn, J. W. Hofstraat and D. M. Bassani, *Org. Lett.*, 2005, **7**, 3409–3412.
20 (*a*) C. Wang, S. Shieh, E. LeGoff and M. G. Kanatzidis, *Macromolecules*, 1996, **29**, 3147–3156; (*b*) C.-J. Yang and S. A. Jenekhe, *Chem. Mater.*, 1991, **3**, 878–887.
21 W. G. Skene and T. Trefz, *Polym. Prepr. (Am. Chem. Soc., Div. Polym. Chem.)*, 2004, **45**, 563–564.
22 M. Bourgeaux, S. A. Perez Guarin and W. G. Skene, *J. Mater. Chem.*, 2006, DOI: 10.1039/b615325a.
23 W. G. Skene and S. Dufresne, *Polym. Prepr. (Am. Chem. Soc., Div. Polym. Chem.)*, 2004, **45**, 728–729.
24 H. W. Boone, J. Bryce, T. Lindgren, A. B. Padias and H. K. J. Hall, *Macromolecules*, 1997, **30**, 2797–2799.
25 (*a*) S. J. Rowan, S. J. Cantrill, G. R. L. Cousins, J. K. M. Sanders and J. F. Stoddart, *Angew. Chem., Int. Ed.*, 2002, **41**, 898–952; (*b*) C. Godoy-Alcántar, A. K. Yatsimirsky and J.-M. Lehn, *J. Phys. Org. Chem.*, 2005, **18**, 979–985; (*c*) J.-M. Lehn, *Prog. Polym. Sci.*, 2005, **30**, 814; (*d*) D. Zhao and J. S. Moore, *Macromolecules*, 2003, **36**, 2712–2720; (*e*) N. Giuseppone and J.-M. Lehn, *Polym. Mater.: Sci. Eng.*, 2004, **90**, 725.
26 N. Giuseppone, J.-L. Schmitt, E. Schwartz and J.-M. Lehn, *J. Am. Chem. Soc.*, 2005, **127**, 5528–5539.
27 (*a*) N. Giuseppone and J.-M. Lehn, *Chem.–Eur. J.*, 2006, **12**, 1723–1735; (*b*) N. Giuseppone and J.-M. Lehn, *Chem.–Eur. J.*, 2006, **12**, 1715–1722.
28 J. F. A. Van Der Looy, G. J. H. Thys, P. E. M. Dieltiens, D. De Schrijver, C. Van Alsenoy and H. J. Geise, *Tetrahedron*, 1997, **53**, 15069–15084.
29 J.-M. Lehn, *Chem.–Eur. J.*, 2006, **12**, 5910–5915.
30 J. Seixas de Melo, F. Elisei, C. Gartner, G. G. Aloisi and R. S. Becker, *J. Phys. Chem. A*, 2000, **104**, 6907–6911.
31 J. Seixas de Melo, F. Elisei and R. S. Becker, *J. Chem. Phys.*, 2002, **117**, 4428–4435.
32 R. S. Becker, J. Seixas de Melo, A. L. Maçanita and F. Elisei, *J. Phys. Chem.*, 1996, **100**, 18683–18695.
33 D. Wasserberg, P. Marsal, S. C. J. Meskers, R. A. J. Janssen and D. Beljonne, *J. Phys. Chem. B*, 2005, **109**, 4410–4415.
34 (*a*) W. Paa, J.-P. Yang and S. Rentsch, *Appl. Phys. B*, 2000, **71**, 443–449; (*b*) H. D. Burrows, L. G. Arnaut, J. Pina, J. Seixas de Melo, N. Chattopadhyay, L. Alcacer, A. Charas and J. Morgado, *Chem. Phys. Lett.*, 2005, **402**, 197–201.
35 (*a*) J. Seixas de Melo, L. M. Silva, L. G. Arnaut and R. S. Becker, *J. Chem. Phys.*, 1999, **111**, 5427–5433; (*b*) J. Seixas de Melo, H. D. Burrows, M. Svensson, M. R. Andersson and A. P. Monkman, *J. Chem. Phys.*, 2003, **118**, 1550–1556.
36 (*a*) L. J. Andrews, A. Deroulede and H. Linschltz, *J. Phys. Chem.*, 1978, **82**, 2304–2309; (*b*) R. S. Murphy, C. P. Moorlag, W. H. Green and C. Bohne, *J. Photochem. Photobiol., A*, 1997, **110**, 123–129.
37 D. Wasserberg, S. P. Dudek, S. C. J. Meskers and R. A. J. Janssen, *Chem. Phys. Lett.*, 2005, **411**, 273–277.
38 J. C. Scaiano, *CRC Handbook of Organic Photochemistry*, CRC Press, Boca Raton, FL, 1989.
39 (*a*) I. Carmichael and G. L. Hug, *J. Phys. Chem. Ref. Data*, 1986, **15**, 1–250; (*b*) I. Carmichael, W. P. Helman and G. L. Hug, *J. Phys. Chem. Ref. Data*, 1987, **16**, 239–260; (*c*) I. Carmichael and G. L. Hug, in *Handbook of Organic Photochemistry*, ed. J. C. Scaiano, CRC Press, Boca Raton, FL, 1989, pp. 369–403.
40 H. Lund and O. Hammerich, *Organic Electrochemistry*, Marcel Dekker, New York, 2001.
41 T. V. D. P. Rao, G. Veerabhadram and K. S. Sastry, *J. Electrochem. Soc. India*, 2001, **50**, 68–71.
42 (*a*) R. W. Koch and R. E. Dessy, *J. Org. Chem.*, 1982, **47**, 4452–4459; (*b*) B. Soucaze-Guillous and H. Lund, *J. Electroanal. Chem.*, 1997, **423**, 109–114.
43 M. M. Baizer and H. Lund, *Organic Electrochemistry: An Introduction and A Guide*, Marcel Dekker, Inc., New York, 1983.
44 R. A. Gavar, Y. P. Stradyn, M. B. Fleisher, V. P. Kadysh and V. A. Slavinskaya, *Theor. Exp. Chem.*, 1981, **16**, 267–270.
45 A. K. Agrawal and S. A. Jenekhe, *Chem. Mater.*, 1996, **8**, 579–589.
46 Even though a suitable analogue for spectroscopic and electrochemical data comparison should contain an electron withdrawing group similar to **1**, there are no literature examples for such derivatives of **23**.
47 (*a*) C. I. Simionescu, I. Cianga, M. Ivanoiu, A. Duca, I. Cocarla and M. Grigoras, *Eur. Polym. J.*, 1999, **35**, 587–599; (*b*) F. R. Diaz, M. A. del Valle, F. Brovelli, L. H. Tagle and J. C. Bernede, *J. Appl. Polym. Sci.*, 2003, **89**, 1614–1621.
48 J. Roncali, *Chem. Rev.*, 1992, **92**, 711–738.
49 (*a*) A. Caballero, A. Tárraga, M. D. Velasco and P. Molina, *Dalton Trans.*, 2006, 1390–1398; (*b*) M. Higuchi and K. Yamamoto, *Polym. Adv. Technol.*, 2002, **13**, 765–770; (*c*) O. Catanescu, M. Grigoras, G. Colotin, A. Dobreanu, N. Hurduc and C. I. Simionescu, *Eur. Polym. J.*, 2001, **37**, 2213–2216; (*d*) M. Grigoras, C. O. Catanescu and G. Colotin, *Macromol. Chem. Phys.*, 2001, **202**, 2262–2266.
50 (*a*) C. Jérôme, C. Maertens, M. Mertens, R. Jérôme, C. Quattrocchi, R. Lazzaroni and J. L. Brédas, *Synth. Met.*, 1996, **83**, 103–109; (*b*) C. Jérôme, C. Maertens, M. Mertens, R. Jérôme, C. Quattrocchi, R. Lazzaroni and J. L. Brédas, *Synth. Met.*, 1997, **84**, 163–164; (*c*) J. A. E. H. v. Haare, E. E. Havinga, J. L. J. v. Dongen, R. A. J. Janssen, J. Cornil and J.-L. Brédas, *Chem.–Eur. J.*, 1998, **4**, 1509–1522.
51 W. G. Skene, S. Dufresne, T. Trefz and M. Simard, *Acta Crystallogr., Sect. E*, 2006, **62**, o2382–o2384.

52 S. Dufresne, M. Bourgeaux and W. G. Skene, *Acta Crystallogr., Sect. E*, 2006, **62**, o5602–o5604.
53 W. G. Skene and T. Trefz, *Polym. Mater.: Sci. Eng.*, 2004, **91**, 326–327.
54 M. Grigoras and C. O. Catanescu, *J. Macromol. Sci., Polym. Rev.*, 2004, **C44**, 131–173.
55 W. G. Skene and S. Dufresne, *Acta Crystallogr., Sect. E*, 2006, **62**, o1116–o1117.
56 (*a*) P. Blanchard, H. Brisset, B. Illien, A. Riou and J. Roncali, *J. Org. Chem.*, 1997, **62**, 2401–2408; (*b*) G. Ruban and D. Zobel, *Acta Crystallogr., Sect. B*, 1975, **31**, 2632–2634.
57 (*a*) E. H. Elandaloussi, P. Frère, P. Richomme, J. Orduna, J. Garin and J. Roncali, *J. Am. Chem. Soc.*, 1997, **119**, 10774–10784; (*b*) I. Jestin, P. Frère, P. Blanchard and J. Roncali, *Angew. Chem., Int. Ed.*, 1998, **37**, 942–945.
58 R. Gawinecki and F. Muzalewski, *Pol. J. Chem.*, 1984, **58**, 1091–1098.
59 N. J. Coville and E. W. Neuse, *J. Org. Chem.*, 1977, **42**, 3485–3491.
60 A. Facchetti, M.-H. Yoon, C. L. Stern, G. R. Hutchison, M. A. Ratner and T. J. Marks, *J. Am. Chem. Soc.*, 2004, **126**, 13480–13501.